Confirmation of ^{123}I-FP-CIT SPECT Quantification Methods in Dementia with Lewy Bodies and Other Neurodegenerative Disorders

Daniela D. Maltais[1], Lennon G. Jordan[1], Hoon-Ki Min[1], Toji Miyagawa[2], Scott A. Przybelski[3], Timothy G. Lesnick[3], Robert R. Reichard[4], Dennis W. Dickson[5], Melissa E. Murray[5], Kejal Kantarci[1], Bradley F. Boeve[2], and Val J. Lowe[1]

[1]Department of Radiology, Mayo Clinic, Rochester, Minnesota; [2]Department of Neurology, Mayo Clinic, Rochester, Minnesota; [3]Department of Health Sciences Research, Mayo Clinic, Rochester, Minnesota; [4]Department of Anatomic Pathology, Mayo Clinic, Rochester, Minnesota; and [5]Department of Neuroscience, Mayo Clinic, Jacksonville, Florida

Our rationale was to conduct a retrospective study comparing 3 ^{123}I-*N*-ω-fluoropropyl-2β-carbomethoxy-3β-(4-iodophenyl)nortropane (^{123}I-FP-CIT) SPECT quantitative methods in patients with neurodegenerative syndromes as referenced to neuropathologic findings. **Methods:** ^{123}I-FP-CIT-SPECT and neuropathologic findings among patients with neurodegenerative syndromes from the Mayo Alzheimer Disease Research Center and Mayo Clinic Study of Aging were examined. Three ^{123}I-FP-CIT SPECT quantitative assessment methods —MIMneuro, DaTQUANT, and manual region-of-interest creation on a workstation—were compared with neuropathologic findings describing the presence or absence of Lewy body disease (LBD). Striatum-to-background ratios (SBRs) generated by DaTQUANT were compared with the calculated SBRs of the manual method and MIMneuro. The left and right SBRs for caudate, putamen, and striatum were evaluated with the manual method. For DaTQUANT and MIMneuro, the left, right, total, and average SBRs and *z* scores for whole striatum, caudate, putamen, anterior putamen, and posterior putamen were calculated. **Results:** The cohort included 24 patients (20 [83%] male, mean age for all patients at death, 75.4 ± 10.0 y). The antemortem clinical diagnoses were Alzheimer disease dementia ($n = 6$), probable dementia with Lewy bodies ($n = 12$), mixed Alzheimer disease dementia and probable dementia with Lewy bodies ($n = 1$), Parkinson disease with mild cognitive impairment ($n = 2$), corticobasal syndrome ($n = 1$), idiopathic rapid-eye-movement sleep behavior disorder ($n = 1$), and behavioral-variant frontotemporal dementia ($n = 1$). Seventeen (71%) had LBD. All 3 ^{123}I-FP-CIT SPECT quantitative methods had an area under the receiver-operating-characteristics curve ranging from more than 0.93 to up to 1.000 ($P < 0.001$) and showed excellent discrimination between LBD and non-LBD patients in each region assessed ($P < 0.001$). There was no significant difference between the accuracy of the regions in discriminating the 2 groups, with good discrimination for both caudate and putamen. **Conclusion:** All 3 ^{123}I-FP-CIT SPECT quantitative methods showed excellent discrimination between LBD and non-LBD patients in each region assessed, using both SBRs and *z* scores.

Key Words: dementia with Lewy bodies; Lewy body disease; ^{123}I-FP-CIT SPECT; ^{123}I-ioflupane; neuropathology

J Nucl Med 2020; 61:1628–1635
DOI: 10.2967/jnumed.119.239418

Dementia with Lewy bodies (DLB) is a neurodegenerative disorder clinically characterized by dementia associated with varying degrees of parkinsonism, cognitive fluctuations, recurrent visual hallucinations, and idiopathic rapid-eye-movement sleep behavior disorder (iRBD) (*1*). Probable DLB (pDLB), the dementia syndrome usually associated with underlying Lewy body disease (LBD), is the second most common type of degenerative dementia in the older adult population after Alzheimer disease dementia (ADem) (*2*). The combination of degenerative motor and cognitive functions contributes to a higher mortality rate and greater use of resources in pDLB patients than in ADem patients with a similar symptom severity (*3,4*). Many challenges relating to pDLB exist and have persisted for decades, particularly the difficulty in accurately predicting LBD before death among those with dementia (*5*).

Challenges in diagnosis have arisen for 3 main reasons (*5*). First, there are few valid and reliable methods to assess core clinical features such as fluctuating cognition and visual hallucinations (*5*). Second, there are discrepancies between autopsy findings and the presentation of core clinical features. Third, the clinical and pathologic overlap between pDLB and ADem, Parkinson disease, vascular dementia, and frontotemporal lobar degeneration (FTLD) make these syndromes hard to discriminate; their common coexistence adds yet another layer of complexity and makes the accuracy of reliance on clinical presentation alone imperfect (*6*). For these reasons, indicative biomarkers were proposed to support the clinical suspicion of pDLB based on core features alone (*5*).

^{123}I-*N*-ω-fluoropropyl-2β-carbomethoxy-3β-(4-iodophenyl)nortropane (^{123}I-FP-CIT) SPECT, an indicative biomarker of pDLB, is currently one of the most widely used probes for imaging dopamine transporters (*7,8*). One study demonstrated a strong correlation between abnormal ^{123}I-FP-CIT SPECT binding and LBD (*7*), and other studies suggested that ^{123}I-FP-CIT SPECT has 70%–80% sensitivity for diagnosing clinical pDLB and more than 80% specificity for excluding non-pDLB neurodegenerative syndromes (*7*).

Received Nov. 15, 2019; revision accepted Mar. 16, 2020.
For correspondence or reprints contact: Val J. Lowe, Department of Radiology, Mayo Clinic, 200 First St., S.W., Rochester, MN 55905.
E-mail: vlowe@mayo.edu
Published online Mar. 20, 2020.

Currently, ^{123}I-FP-CIT SPECT is often interpreted in clinical practice using only qualitative visual interpretation. However, there are several possible limitations when solely qualitative visual inspection is relied on for interpretation (*8*). Subtle changes in the striatum or its specific subregions may be problematic on visual inspection, and high reproducibility may be a challenge in longitudinal studies (*8*). For these reasons, automated, semiautomated, and manual quantitative methods for ^{123}I-FP-CIT SPECT could be helpful (*8,9*).

Ratios that compare the ^{123}I-FP-CIT SPECT radiopharmaceutical uptake to a reference region of low dopamine transporter density are used in quantitative analyses (*7*). Some software programs may give options to manually position regions of interest (ROIs) on the images; however, this procedure is time-consuming and leads to intrarater and interrater variability (*10*). Automated and semiautomated quantitative methods that have predefined ROIs in a normalized space are more time-efficient; however, if the predefined ROIs are not based on individual morphology, the results may still be skewed in patients for whom a low specific binding is expected (*11*). More success in the clinical diagnosis of dementia has been found when individual-patient images were compared with a normative database that provided *z* score maps, which compensate for age and sex effects (*12*).

Several quantification methods are available, including DaTQUANT (GE Healthcare) (*9*), MIMneuro (MIM Software Inc.) (*13*), and manual ROI creation on an Advantage Workstation (GE Healthcare) (*7*). In this study, we paired neuropathologic findings and clinical data to investigate the comparative diagnostic accuracy of these quantification methods for predicting LBD versus non-LBD.

MATERIALS AND METHODS

Participants

Participants with neurodegenerative syndromes from the Mayo Clinic Alzheimer Disease Research Center and the Mayo Clinic Study of Aging were examined. The inclusion criteria were as follows: a diagnosis of a neurodegenerative syndrome, analyzable ^{123}I-FP-CIT SPECT images, and autopsy with neuropathologic examination. Published criteria enabled the consensus clinical diagnoses of a neurodegenerative syndrome, including ADem (*14*), pDLB (*1*), mixed ADem and pDLB, Parkinson disease with mild cognitive impairment (*15*), corticobasal syndrome (*16*), FTLD (*17*), and iRBD (*18*). Polysomnography was used to confirm rapid-eye-movement sleep without atonia, which is required for a diagnosis of definite iRBD. Mayo institutional review board approval was granted, and informed consent was given by the patients or their proxies.

^{123}I-FP-CIT SPECT Acquisitions

At least 1 h before the injection of ^{123}I-FP-CIT, a 100-mg Lugol solution was given, and then the recommended intravenous ^{123}I-FP-CIT dose of 111–185 MBq (3–5 mCi) was administered slowly. ^{123}I-FP-CIT SPECT was performed 3.2 ± 1.9 y before death in patients with pDLB and 2.4 ± 1.6 y before death in patients without pDLB. SPECT imaging occurred 3–6 h after injection. A GE Healthcare D670 or D630 SPECT system with ultra-high-resolution fan-beam collimators and an energy setting of 159 keV with a 20% window was used on all patients. Data were reconstructed using ordered-subset expectation maximization, and the planar images were prefiltered using a Butterworth filter (power, 10; cutoff, 0.6 cycles/cm), and no attenuation correction was used. For DaTQuant, we used projection images as input. Case study SPECT images were coregistered with MR images using the VINCI software program (Max Planck Institute, Cologne, Germany), provided by the Max Planck Institute.

Imaging Analysis

The presence or absence of LBD confirmed by neuropathologic findings was compared against results from 3 ^{123}I-FP-CIT SPECT quantitative methods: MIMneuro, DaTQUANT, and manual ROI creation on an Advantage Workstation. Selection of the best representative slide and placement of the ROIs was done in the manual method, and then the left and right striatum-to-background ratios (SBRs) for caudate, putamen, and striatum were calculated using the following formula:

$$\frac{\text{Right caudate mean}}{\text{Average of the left and right occipital mean}} - 1 = \text{SBR for right caudate.}$$

MIMneuro calculated the *z* scores for the left and right striatum, caudate, putamen, anterior putamen, and posterior putamen. The SBRs for these regions were manually calculated using a formula similar to the one above. The left, right, and average *z* scores and SBRs for the same regions were calculated by DaTQUANT. MIMneuro had 3 cases of coregistration error, and these were subsequently discarded. For the analysis, each left and right SBR and *z* score was reclassified for ranking purposes; the lowest value was labeled as the minimum, the highest value was labeled as the maximum, and the average of the minimum and maximum was labeled as the average.

Neuropathologic Methods

The neuropathologists did not know the ^{123}I-FP-CIT SPECT results and relied on previously published neuropathologic assessments. Of these, we used Braak staging criteria (*19,20*), Consortium to Establish a Registry for Alzheimer Disease scores (*21*), Thal Aβ phases (*22*), LBD pathologic criteria (*1*), and FTLD classification (*23*).

Statistical Methods

Analysis of variance for continuous variables and a χ^2 test for categoric variables were used to test for differences in characteristics among 3 groups: the LBD group, the LBD and Alzheimer disease (AD) group, and the no-LBD group. Area under the receiver-operating-characteristics curve (AUC) was used to test for neuropathologic group discrimination for the various semiquantitative image analysis programs. Intraclass correlation coefficients were used to assess the relationship between the image analysis programs and ROIs. Because of the differences in scales, the less stringent consistency approach was applied. Box-and-whisker plots displayed the distribution of ROIs (in *z* score and SBR format) and their relation to neuropathologic diagnosis. The reported cutoffs on the box plots were based on the Youden method, which maximizes the distance in relation to the identity line. Additional testing was performed using ANOVA with contrast statements for pairwise comparisons. All these analyses considered a *P* value of less than 0.05 as statistically significant.

RESULTS

Participants

Twenty-four patients met the inclusion criteria, of whom 11 had pathologic confirmation of LBD, 6 had a mixture of LBD and AD, and 7 had no LBD (6 AD and 1 FTLD). A sensitivity analysis was run with the FTLD participant excluded, and the results remained essentially the same. The demographic, clinical, pathologic, and ^{123}I-FP-CIT SPECT characteristics of these patients are summarized in Supplemental Table 1 (supplemental materials are available at http://jnm.snmjournals.org). For these patients, the mean onset of cognitive decline was at the age of 65.9 ± 9.1 y. Twenty (83%)

patients were male, and the mean age for all patients at death was 75.4 ± 10.0 y. The antemortem clinical diagnoses were ADem (n = 6), pDLB (n = 12), mixed ADem and pDLB (n = 1), Parkinson disease plus mild cognitive impairment (n = 2), corticobasal syndrome (n = 1), iRBD (n = 1), and FTLD (n = 1). Seventeen patients (71%) had LBD confirmed by neuropathologic examination. Most (22/24) of the clinical diagnoses at the time of imaging were in concordance with the neuropathologic findings. Clinical scales, such as the Boston Naming Test (P = 0.10) (*24*), Global Deterioration Scale (P = 0.22) (*25*), and Trail-Making Test, Part A (P = 0.14) (*26*), were examined for differences and were not found to be statistically significant. MMSE (P = 0.003) (*27*) and the Category Fluency Total (P = 0.031) (*28*) were found to be significant. Variables such as apolipoprotein E4 (P = 0.27), time from scan date to death (P = 0.60), and education (P = 0.33) were not significant. On the other hand, sex (P = 0.036), age when the patient was scanned (P = 0.029), and age at patient death (P = 0.028) were significant.

Imaging Analysis

The mean age at which ^{123}I-FP-CIT SPECT was performed for all patients was 72.4 ± 9.5 y, and a mean of 3.0 ± 1.8 y represents the time between scan and death. Each possible ROI SBR and z score generated by the 3 quantitative methods was compared against neuropathologic data. The AUC analysis demonstrated excellent group discrimination between LBD and non-LBD patients for each program and each tested ROI (Fig. 1). The range for all AUCs was 0.93–1.000 ($P < 0.001$). Of note, the caudate minimum z score achieved a 1.00 AUC or perfect group separation. The SBRs and z scores for all ROIs across all image analysis programs were ranked from greatest to least; the highest numeric AUCs corresponded mainly to the minimum caudate, followed by the minimum striatum across all programs and scores. The 2 × 2 AUC in Supplemental Figure 1 demonstrates the overlap found in each program across the minimum striatum, minimum caudate, and minimum putamen and the overlap found between programs. Diagnoses derived from visual inspection alone were compared against neuropathologic data. The AUC for this analysis was 0.971 (95% confidence interval, 0.753–0.997).

The analysis of intraclass correlation coefficients for the image analysis programs showed strong associations: the correlation between DaTQUANT SBR and manual SBR was r = 0.913 ($P <$ 0.001) for the caudate, r = 0.898 ($P < 0.001$) for the putamen, and r = 0.920 ($P <$ 001) for the striatum. Similar trends were evident, although slightly lower, between the DaTQUANT z score and MIMneuro z score, at r = 0.811 ($P < 0.001$) for the caudate, r = 0.856 ($P < 0.001$) for the putamen, and r = 0.855 ($P < 0.001$) for the striatum (Fig. 2). Across all image analysis programs and ROIs, group separation of LBD versus no LBD was evident in box-and-whisker plots (Fig. 3). Optimal cutoffs are delineated in red in Figure 3 and numerically shown in Supplemental Table 2. ANOVA models with contrast statements showed—in testing of pairwise comparisons—that the striatum, caudate, and putamen quantified through DaTQUANT SBRs, through DaTQUANT z scores, and manually were different in 2 neuropathologic categories: AD versus LBD ($P < 0.001$) and AD versus mixed LBD and AD ($P < 0.001$). MIM z score was also significantly different in these categories ($P < 0.05$). All 3 quantitative image analysis

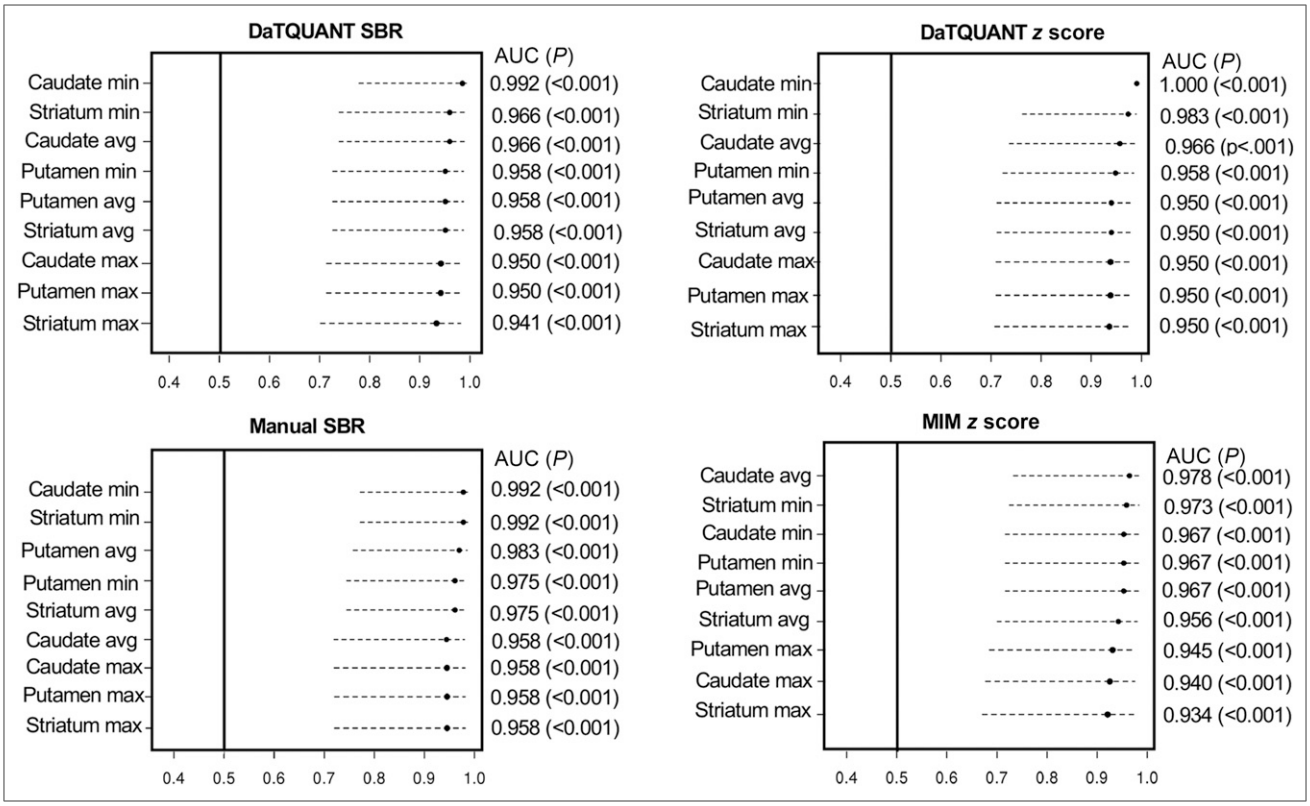

FIGURE 1. Diagnostic accuracy using AUC of SBR and z scores for various ROIs as calculated by MIM, by DaTQUANT, and manually to differentiate between no LBD and LBD.

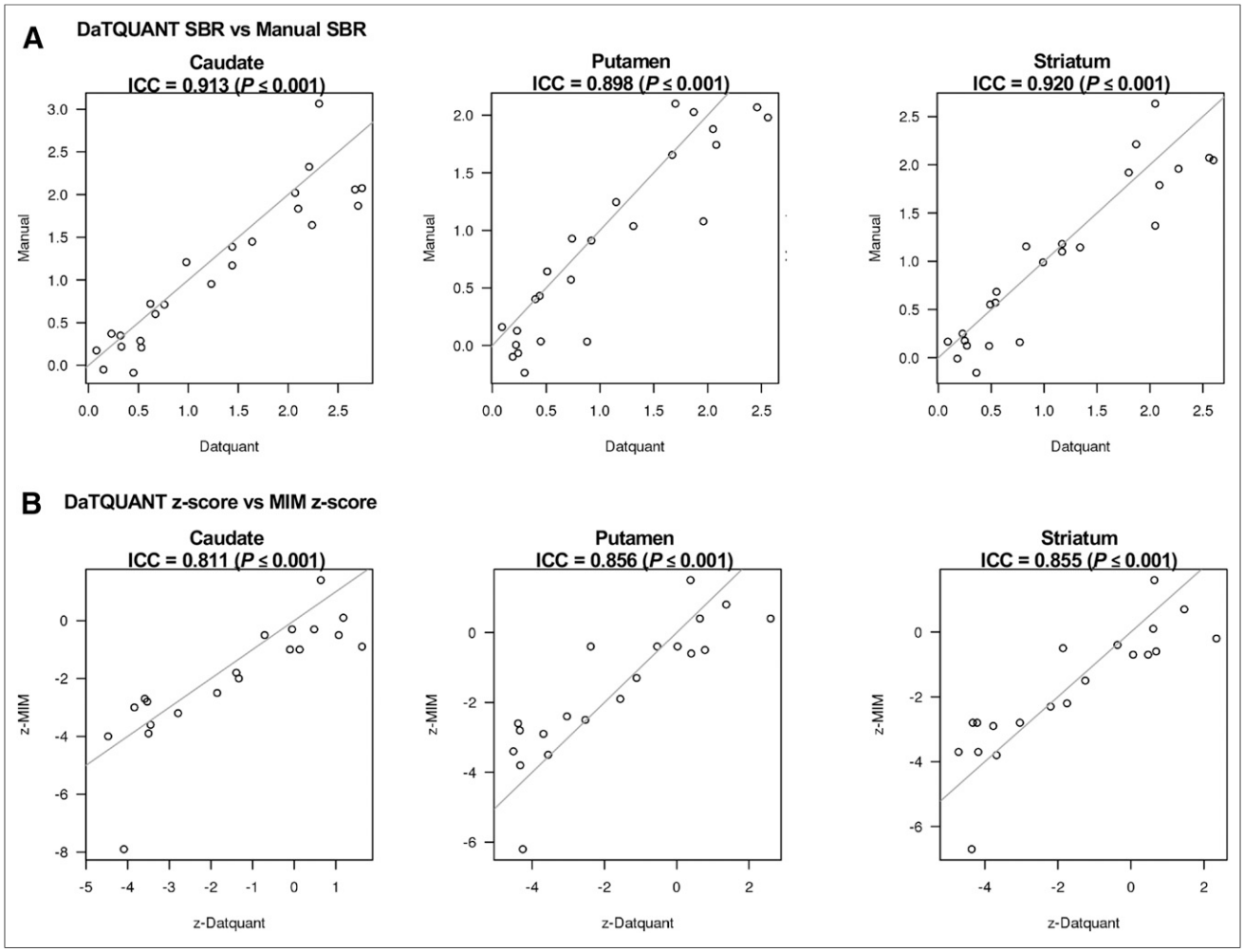

FIGURE 2. Correlations between programs using minimum caudate, minimum putamen, and minimum striatum SBRs (A) and *z* scores (B). ICC = intraclass correlation coefficient.

programs showed no differences between patients with LBD and patients with mixed LBD and AD ($P < 0.23$) (Supplemental Table 3).

Case Studies

Six patients highlighted the utility and limitations of ^{123}I-FP-CIT SPECT (Fig. 4). Patient 1 was a 75-y-old woman clinically diagnosed with ADem. ^{123}I-FP-CIT SPECT had abnormal results, and neuropathologic examination revealed diffuse LBD and AD with a Braak stage of VI. In this patient, ^{123}I-FP-CIT SPECT was able to detect profound abnormality in the midbrain despite a clinical presentation that resembled ADem. Patient 2 was a 55-y-old man clinically diagnosed with ADem and pDLB. The ^{123}I-FP-CIT SPECT results were normal, and neuropathologic examination revealed no LBD but AD with a Braak stage of VI. In this patient, the dual clinical diagnosis disagreed with the single type of neuropathologic disease found (AD). ^{123}I-FP-CIT SPECT interpretation and neuropathologic examination agreed, with high SBRs ranging from 2.56 to 2.74. Patient 3 was a 63-y-old woman clinically diagnosed with ADem. ^{123}I-FP-CIT SPECT had normal results, and neuropathologic examination revealed diffuse LBD. Although LBs were present in the substantia nigra and in limbic and neocortical structures, the high SBRs (1.98–2.10) suggest that the degenerative changes in the nigrostriatal system were relatively mild and below the threshold of detection by ^{123}I-FP-CIT SPECT imaging. Patient 4 was a 59-y-old man clinically diagnosed with ADem. ^{123}I-FP-CIT SPECT had normal results, and neuropathologic examination revealed AD with a Braak stage of V. This was an example of a typical case of AD; agreement existed between the clinical diagnosis,^{123}I-FP-CIT SPECT, and neuropathologic examination. Patient 5 was a 74-y-old man clinically diagnosed with ADem. ^{123}I-FP-CIT SPECT had normal results, and neuropathologic examination revealed AD with amygdala-restricted Lewy bodies and Braak stage VI. These cases of amygdala-only LBD tend to occur in advanced AD and are not viewed as reflecting typical LBD. Patient 6 was a 77-y-old man clinically diagnosed with pDLB. ^{123}I-FP-CIT SPECT results were abnormal, and neuropathologic examination revealed diffuse LBD, vascular dementia, and pathologic aging. ^{123}I-FP-CIT SPECT provided low SBR scores of 1.17 and 1.64, matching the clinical diagnosis of pDLB. MRI-coregistered images that match the summary information in Table 1 and the neuropathologic information in Table 2 are presented in Figure 4.

DISCUSSION

We examined the relationship between neuropathologic findings and 3 semiquantitative ^{123}I-FP-CIT SPECT image analysis programs

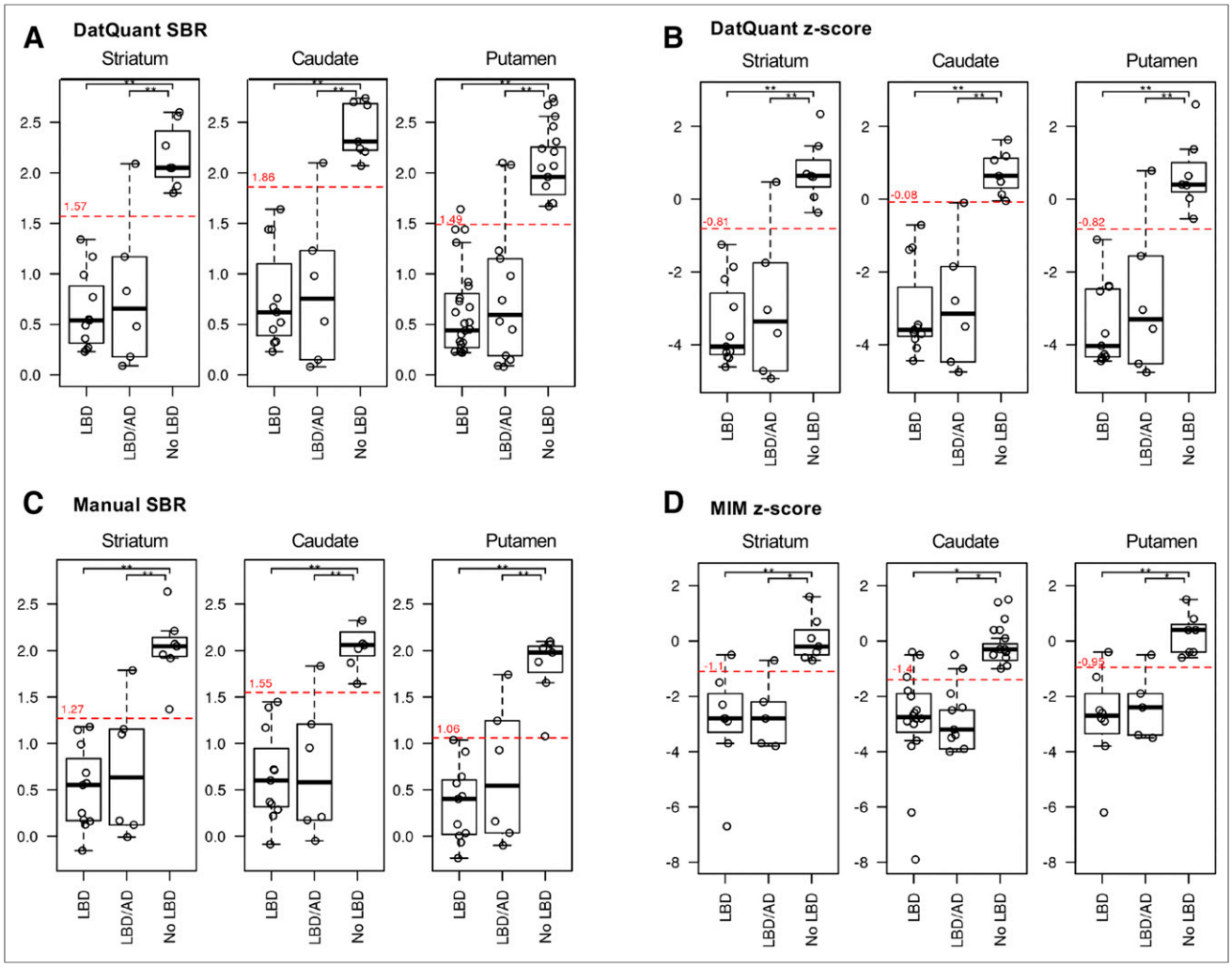

FIGURE 3. Box-and-whisker plots showing distribution of *z* scores and SBRs for minimum striatum, minimum caudate, and minimum putamen among LBD, mixed LBD and AD, and no-LBD neuropathologic diagnoses. *$0.001 < P < 0.05$. **$P < 0.001$.

in a cohort of 24 patients. All 3 ^{123}I-FP-CIT SPECT quantitative methods showed excellent discrimination between LBD and non-LBD patients in each region assessed using both SBRs and *z* scores. Positive correlations were seen between programs and their respective *z* scores in the caudate, putamen, and striatum.

The combination of neuropathologic findings (considered the gold standard) and clinical data has been shown to provide a more robust assessment of the role ^{123}I-FP-CIT SPECT plays in the diagnosis of pDLB (*29*). Several studies reported enhanced sensitivity and specificity from using ^{123}I-FP-CIT SPECT over using clinical criteria alone, when both were paired with neuropathologic data (*30,31*). In one such study, the ability of ^{123}I-FP-CIT SPECT to indicate LBD had a sensitivity of 88% and a specificity of 100%, whereas clinical criteria alone had a 75% specificity and 42% sensitivity (*31*).

In our study, both visual inspection and semiquantification assessment of ^{123}I-FP-CIT SPECT showed good concordance with neuropathologic results. Of the 17 confirmed cases of LBD, visual inspection alone was able to detect abnormality in 16. (The single missed case is shown as case 3 in Fig. 4). However, the below-cutoff minimum caudate *z* score (derived from quantification) corrected this false-negative. Mixed diffuse LBD and AD was confirmed in 6 patients. Of these 6 patients, 4 were clinically diagnosed with pDLB and 2 with ADem. One of the 6 patients with mixed LBD and AD pathology had a false-negative ^{123}I-FP-CIT SPECT result (based on the DLB pathology). Among the 6 patients who had confirmed cases of mixed LBD and AD, the clinical diagnoses could be explained by any of the following: prominence on the part of one type of neuropathologic disease without clinical observation of other type of neuropathologic disease, leading to the specific classifying symptomatology; overlap of symptoms between pDLB and ADem, causing confusion; or a long time between last clinical evaluation and autopsy. Better characterization of these patients, whether they have mixed diseases or not, may be better refined with multimodality imaging (*32*). Sensitive tools, such as quantification programs used in serial imaging, could be particularly useful to assess specific signal changes over time that could add more confidence. Among the cases of confirmed LBD, one was clinically diagnosed as iRBD and two were clinically diagnosed as Parkinson disease dementia. ^{123}I-FP-CIT SPECT identified these cases as abnormal, and symptoms played a critical role in properly clinically characterizing them.

The utility of ^{123}I-FP-CIT SPECT was highlighted in 2 patients, one clinically diagnosed with ADem (patient 1) and another with

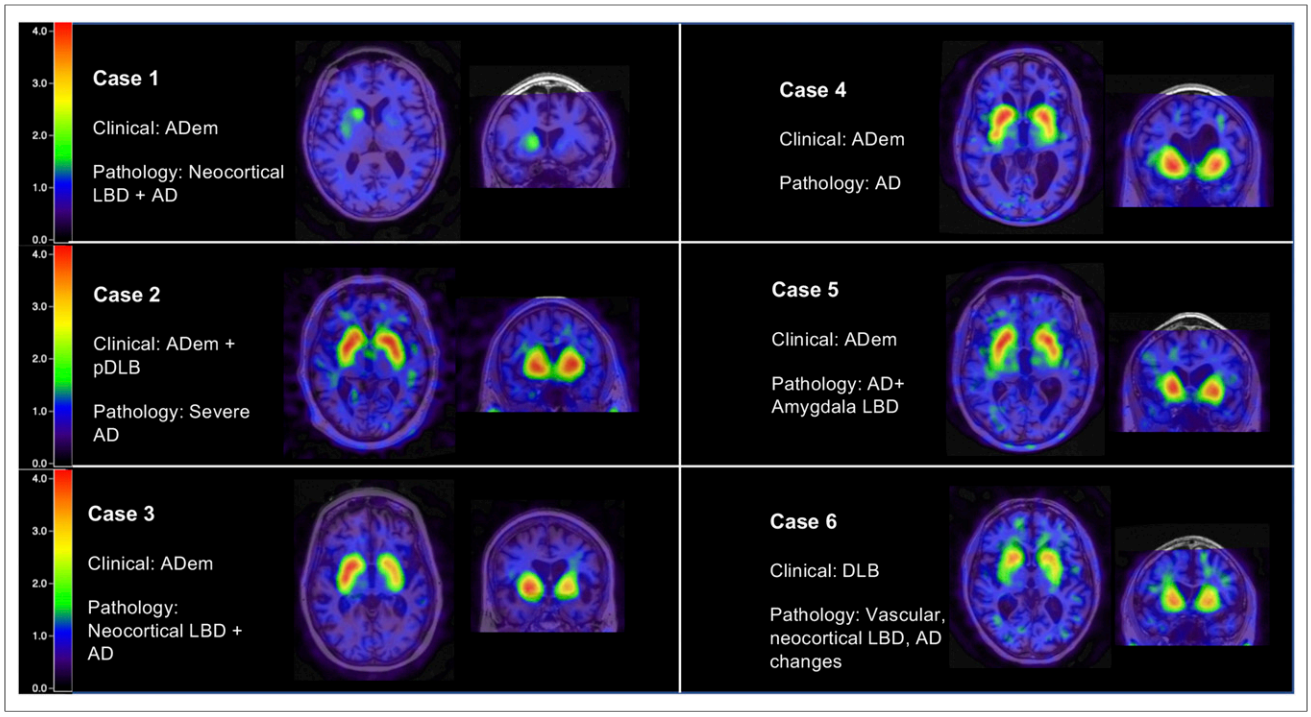

FIGURE 4. Six patients who underwent ^{123}I-FP-CIT SPECT and then neuropathologic examination. Clinical diagnoses before death and pathologic diagnosis are presented alongside each set of MRI coregistered images.

ADem and pDLB (patient 2). In patient 1, ^{123}I-FP-CIT SPECT revealed absence of uptake in the left striatum indicative of LBD. In patient 2, ^{123}I-FP-CIT SPECT showed an intact striatum. These patients show that lower sensitivity in clinical diagnosis can be improved with ^{123}I-FP-CIT SPECT. As such, ^{123}I-FP-CIT SPECT may be particularly helpful when atypical clinical features or diagnostic ambiguities are present (*7*). On the other hand, patients 3 and 5 highlighted the limitation of ^{123}I-FP-CIT SPECT to assess LB in areas outside the striatum. Neuropathologic examination revealed diffuse LBD in patient 3 and AD with amygdala-restricted Lewy bodies in patient 5, whereas ^{123}I-FP-CIT SPECT images of the striatum appeared relatively intact. The lower sensitivity in past ^{123}I-FP-CIT SPECT studies has been hypothesized to occur because of the presence of LBD disease in the limbic structures with or without the neocortical structures but less so in the nigrostriatal system in the early stages of disease (*33*). ^{18}F-FE-PE2I, a novel dopamine transporter tracer, shows promise to discriminate between healthy controls and patients with early Parkinson disease (*34*).

High diagnostic accuracy was found with visual inspection and all 3 quantification programs. Sample size, lack of masking, and experienced observers may have contributed to this finding. This high accuracy contrasts with previous reports that have shown benefits from quantitative programs, such as improving diagnostic accuracy, particularly among residents and less experienced

TABLE 1
Clinical Data, Minimum SBRs, Minimum *z* Scores, and Antemortem and Postmortem Diagnoses for the 6 Patients Who Underwent ^{123}I-FP-CIT SPECT and Then Neuropathologic Examination

Patient no.	Age at scan (y)	Time between last scan and death (y)	SBR						DAT visual interpretation	Clinical diagnosis before death	UPDRS	MMSE	CDR sum of boxes
			DQ		MIM		Manual						
			Striatum	Caudate	Striatum	Caudate	Striatum	Caudate					
1	75	2.23	0.09 (−4.72)	0.08 (−4.47)	0.27 (−3.70)	0.3 (−4.00)	.17	1.17	Abnormal	ADem	7	N/A	13
2	55	2.06	2.56 (1.46)	2.74 (1.18)	2.77 (0.70)	2.7 (0.10)	2.07	3.08	Normal	ADem + pDLB	5	15	3.5
3	63	2.85	2.09 (0.47)	2.10 (−0.10)	1.98 (−0.70)	2.05 (−1.00)	1.79	2.83	Normal	ADem	0	6	9
4	59	2.93	1.87 (−0.37)	2.21 (−0.05)	2.14 (−0.40)	2.37 (−0.30)	2.21	3.32	Normal	ADem	0	14	6
5	74	4.65	1.80 (0.09)	2.07 (0.20)	1.9 (−0.70)	1.89 (−1.00)	1.92	3.02	Normal	ADem (lpvPPA)	0	20	2
6	77	1.05	1.17 (−1.86)	1.64 (−0.71)	1.99 (−0.50)	2.19 (−0.50)	1.18	2.45	Abnormal	pDLB	11	21	6

DQ = DaTQUANT; DAT = ^{123}I-FP-CIT SPECT; UPDRS = Unified Parkinson Disease Rating Scale; MMSE = Mini-Mental State Examination; CDR = Clinical Dementia Rating Staging Instrument; lpvPPA = logopenic variant primary progressive aphasia.

Data in parentheses are *z* scores.

TABLE 2
Clinical and Neuropathologic Data for the 6 Patients Who Underwent ^{123}I-FP-CIT SPECT and Then Neuropathologic Examination

Patient no.	Pathologic diagnosis	Age at death	Sex	Braak stage	NIA-AA	cDLB-4	Midbrain Lewy body involvement
1	Diffuse LBD/AD	78	F	VI	High	Intermediate	Severe to very severe
2	AD	57	M	VI	High	None	None
3	Diffuse LBD	66	F	VI	Intermediate	Intermediate	Mild
4	AD	62	M	V	Intermediate	None	None
5	AD with ALB	78	M	VI	High	Low	None
6	Diffuse LBD/PA/VD	81	M	II	Low	High	Severe to very severe

NIA-AA = National Institute on Aging and Alzheimer Disease guidelines; cDLB-4 = Fourth Consortium on Dementia with Lewy Bodies; ALB = amygdala-restricted Lewy bodies; PA = pathologic aging; VD = vascular dementia.

physicians (*8,35,36*). Quantitative programs have been shown to capture subtle changes that may otherwise pass unobserved (*8*). It is noted that high accuracy was found for the manual semiquantification method, a viable alternative when commercial software programs are not available.

There were some limitations in this study. Differences based on attenuation correction, acquisition collimator, and image reconstruction methods were not assessed. Previous studies have reported, first, higher SBRs when attenuation correction, such as Chang and CT attenuation correction, has been used (*37*) and, second, no difference in diagnostic impact between attenuation-corrected and non–attenuation-corrected images (*38*). Additionally, a comparison between image analysis programs was restricted by the inconsistent data types in the output files. Because of the absence of a reference database, the manual method could not generate *z* scores, thus limiting comparison of *z* scores. From what could be examined, there were no statistical differences between SBRs and *z* scores, and this finding could be influenced by the number of participants and by the matching process used in normative databases. Another potential limitation of our study was the relatively small sample size. However, our findings were strengthened by the similarity of values across programs, as validated by autopsy results.

CONCLUSION

All 3 ^{123}I-FP-CIT SPECT quantitative methods showed excellent discrimination between LBD and non-LBD patients in each region assessed, both through the use of SBRs and through the use of *z* scores. Across all image analysis programs, the SBRs and *z* scores for the minimum caudate and minimum striatum held the highest numeric AUC. Though ^{123}I-FP-CIT SPECT does have a high diagnostic value (as shown here and in the literature), combining these data with clinical and neuropsychologic data is still important (*33,39*).

DISCLOSURE

This work was supported by the National Institutes of Health (U01-NS100620 to Kejal Kantarci and Bradley Boeve, P50-AG016574 to Bradley Boeve, and P30-AG062677), GE Healthcare (Bradley Boeve and Val Lowe), the Mayo Clinic Dorothy and Harry T. Mangurian Jr. Lewy Body Dementia Program, the Deal Family Foundation, the Little Family Foundation, and the Lewy Body Dementia Functional Genomics Program. No other potential conflict of interest relevant to this article was reported.

KEY POINTS

QUESTION: Which ^{123}I-FP-CIT SPECT quantification method, ROI, and score type can best discriminate between LBD and non-LBD patients when paired with neuropathologic confirmation?

FINDINGS: Three ^{123}I-FP-CIT SPECT quantitative assessment methods: MIMneuro, DaTQUANT, and manual ROI creation on an Advantage Workstation, were compared with neuropathologic findings describing the presence or absence of LBD. Using both SBRs and *z* scores, all 3 quantitative methods showed excellent discrimination between LBD and non-LBD patients in each region assessed.

IMPLICATIONS FOR PATIENT CARE: The quantitative image analysis programs studied here highlight the utility of ^{123}I-FP-CIT SPECT to support clinical diagnosis, especially for patients with a complicated presentation, and the potential research scope of quantification when compared with prior reliance on visual inspection alone.

REFERENCES

1. McKeith IG, Boeve BF, Dickson DW, et al. Diagnosis and management of dementia with Lewy bodies: fourth consensus report of the DLB Consortium. *Neurology.* 2017;89:88–100.
2. Zupancic M, Mahajan A, Handa K. Dementia with Lewy bodies: diagnosis and management for primary care providers. *Prim Care Companion CNS Disord.* 2011;13:PCC.11r01190.
3. Williams MM, Xiong CJ, Morris JC, Galvin JE. Survival and mortality differences between dementia with Lewy bodies vs Alzheimer disease. *Neurology.* 2006;67:1935–1941.
4. Boström F, Jonsson L, Minthon L, Londos E. Patients with Lewy body dementia use more resources than those with Alzheimer's disease. *Int J Geriatr Psychiatry.* 2007;22:713–719.
5. McKeith I, O'Brien JT, Walker Z, et al. Sensitivity and specificity of dopamine transporter imaging with ^{123}I-FP-CIT-SPECT in dementia with Lewy bodies: a phase III, multicentre study. *Lancet Neurol.* 2007;6:305–313.
6. Vlaar AM, de Nijs T, Kessels AG, et al. Diagnostic value of ^{123}I-ioflupane and ^{123}I-iodobenzamide SPECT scans in 248 patients with parkinsonian syndromes. *Eur Neurol.* 2008;59:258–266.
7. Jung Y, Jordan LG, Lowe VJ, et al. Clinicopathological and ^{123}I-FP-CIT-SPECT correlations in patients with dementia. *Ann Clin Transl Neurol.* 2018;5:376–381.

8. Augimeri A, Cherubini A, Cascini GL, et al. CADA-computer-aided DaTSCAN analysis. *EJNMMI Phys.* 2016;3:4.
9. Shimizu S, Namioka N, Hirose D, et al. Comparison of diagnostic utility of semi-quantitative analysis for Dat-SPECT for distinguishing DLB from AD. *J Neurol Sci.* 2017;377:50–54.
10. Badiavas K, Molyvda E, Iakovou I, Tsolaki M, Psarrakos K, Karatzas N. SPECT imaging evaluation in movement disorders: far beyond visual assessment. *Eur J Nucl Med Mol Imaging.* 2011;38:764–773.
11. Darcourt J, Booij J, Tatsch K, et al. EANM procedure guidelines for brain neurotransmission SPECT using ^{123}I-labelled dopamine transporter ligands, version 2. *Eur J Nucl Med Mol Imaging.* 2010;37:443–450.
12. Minoshima S, Frey KA, Koeppe RA, Foster NL, Kuhl DE. A diagnostic approach in Alzheimer's disease using three-dimensional stereotactic surface projections of fluorine-18-FDG PET. *J Nucl Med.* 1995;36:1238–1248.
13. Partovi S, Yuh R, Pirozzi S, et al. Diagnostic performance of an automated analysis software for the diagnosis of Alzheimer's dementia with ^{18}F-FDG-PET. *Am J Nucl Med Mol Imaging.* 2017;7:12–23.
14. McKhann GM, Knopman DS, Chertkow H, et al. The diagnosis of dementia due to Alzheimer's disease: recommendations from the National Institute on Aging–Alzheimer's Association workgroups on diagnostic guidelines for Alzheimer's disease. *Alzheimers Dement.* 2011;7:263–269.
15. Litvan I, Goldman JG, Tröster AI, et al. Diagnostic criteria for mild cognitive impairment in Parkinson's disease: Movement Disorder Society Task Force guidelines. *Mov Disord.* 2012;27:349–356.
16. Boeve BF, Lang AE, Litvan I. Corticobasal degeneration and its relationship to progressive supranuclear palsy and frontotemporal dementia. *Ann Neurol.* 2003;54(suppl):S15–S19.
17. Rascovsky K, Hodges JR, Knopman D, et al. Sensitivity of revised diagnostic criteria for the behavioural variant of frontotemporal dementia. *Brain.* 2011;134:2456–2477.
18. Dauvilliers Y, Schenck CH, Postuma RB, et al. REM sleep behaviour disorder. *Nat Rev Dis Primers.* 2018;4:19.
19. Hyman BT, Phelps CH, Beach TG, et al. National Institute on Aging–Alzheimer's Association guideline for the neuropathologic assessment of Alzheimer's disease. *Alzheimers Dement.* 2012;8:1–13.
20. Braak H, Braak E. Neuropathological staging of Alzheimer-related changes. *Acta Neuropathol (Berl).* 1991;82:239–259.
21. Mirra SS, Heyman A, McKeel D, et al. The Consortium to Establish a Registry for Alzheimer's Disease (CERAD). Part II. Standardization of the neuropathologic assessment of Alzheimer's disease. *Neurology.* 1991;41:479–486.
22. Thal DR, Rub U, Orantes M, Braak H. Phases of A-beta deposition in the human brain and its relevance for the development of AD. *Neurology.* 2002;58:1791–1800.
23. Mackenzie IR, Neumann M, Bigio EH, et al. Nomenclature and nosology for neuropathologic subtypes of frontotemporal lobar degeneration: an update. *Acta Neuropathol (Berl).* 2010;119:1–4.
24. Williams BW, Mack W, Henderson VW. Boston naming test in Alzheimer's disease. *Neuropsychologia.* 1989;27:1073–1079.
25. Reisberg B, Ferris SH, de Leon MJ, Crook T. The global deterioration scale for assessment of primary degenerative dementia. *Am J Psychiatry.* 1982;139:1136–1139.
26. Reitan R. Validity of the trail-making test as an indication of organic brain damage. *Percept Mot Skills.* 1958;8:271–276.
27. Folstein MF, Folstein SE, McHugh PR. "Mini-mental state". A practical method for grading the cognitive state of patients for the clinician. *J Psychiatr Res.* 1975;12:189–198.
28. Cerhan JH, Ivnik RJ, Smith GE, Tangalos EC, Peterson RC, Boeve BF. Diagnostic utility of letter fluency, category fluency, and fluency difference scores in Alzheimer's disease. *Clin Neuropsychol.* 2002;16:35–42.
29. Sonni I, Ratib O, Boccardi M, et al. Clinical validity of presynaptic dopaminergic imaging with ^{123}I-ioflupane and noradrenergic imaging with ^{123}I-MIBG in the differential diagnosis between Alzheimer's disease and dementia with Lewy bodies in the context of a structured 5-phase development framework. *Neurobiol Aging.* 2017;52:228–242.
30. Thomas AJ, Attems J, Colloby SJ, et al. Autopsy validation of ^{123}I-FP-CIT dopaminergic neuroimaging for the diagnosis of DLB. *Neurology.* 2017;88:276–283.
31. Walker Z, Jaros E, Walker RW, et al. Dementia with Lewy bodies: a comparison of clinical diagnosis, FP-CIT single photon emission computed tomography imaging and autopsy. *J Neurol Neurosurg Psychiatry.* 2007;78:1176–1181.
32. Kantarci K, Lowe VJ, Boeve BF, et al. Multimodality imaging characteristics of dementia with Lewy bodies. *Neurobiol Aging.* 2012;33:2091–2105.
33. Papathanasiou ND, Boutsiadis A, Dickson J, Bomanji JB. Diagnostic accuracy of ^{123}I-FP-CIT (DaTSCAN) in dementia with Lewy bodies: a meta-analysis of published studies. *Parkinsonism Relat Disord.* 2012;18:225–229.
34. Delva A, Van Weehaeghe D, Van Aalst J, et al. Quantification and discriminative power or ^{18}F-FE-PE2I PET in patients with Parkinson's disease. *Eur J Nucl Med Mol Imaging.* November 27, 2019 [Epub ahead of print].
35. Jiang Y, Nishikawa RM, Schmidt RA, Toledano AY, Doi K. Potential of computer-aided diagnosis to reduce variability in radiologists' interpretations of mammograms depicting microcalcifications. *Radiology.* 2001;220:787–794.
36. Tang BN, Minoshima S, George J, et al. Diagnosis of suspected Alzheimer's disease is improved by automated analysis of regional cerebral blood flow. *Eur J Nucl Med Mol Imaging.* 2004;31:1487–1494.
37. Lange C, Seese A, Schwarzenbock S, et al. CT-Based attenuation correction in I-123-ioflupane-SPECT. *PLoS One.* 2014;9:e108328.
38. Akahoshi M, Abe K, Uchiyama Y, et al. Attenuation and scatter correction in I-123 FP-CIT SPECT do not affect the clinical diagnosis of dopaminergic system neurodegeneration. *Medicine (Baltimore).* 2017;96:e8484.
39. Yeo JM, Lim X, Khan Z, Pal S. Systematic review of the diagnostic utility of SPECT imaging in dementia. *Eur Arch Psychiatry Clin Neurosci.* 2013;263:539–552.